diphosphonate ligands is the orientation of the $-PO_3$ groups with respect to the P–C–P plane. The "W" configuration, wherein the atoms O(2)–P(1)–C–P(2)–O(4) form a planar "W", has been previously described[17,19] and can easily be seen in Figure 1. This configuration allows the ligand to be doubly bidentate with O(1) and O(6) on one side of the "W" coordinating to one metal center and O(3) and O(5) on the other side of the "W" coordinating to another metal center.

The salient structural characteristic of the Tc–MDP complex is its polymeric nature, and it seems likely that polymeric metal–diphosphonate complexes play a central role in the chemistry of technetium–diphosphonate skeletal imaging agents. The propensity of diphosphonates to form polymeric complexes presumably arises from the ability of these ligands to function minimally as doubly bidentate bridges, as for example in Figure 1 where MDP bridges two technetium centers. If the diphosphonate ligand contains a suitable functional group on the central carbon atom (e.g., the hydroxyl group of HEDP) then the diphosphonate can function as a mixed bidentate–tridentate bridge. It has been postulated[17] that the additional hydroxyl group in ligands such as HEDP (relative to MDP which has no hydroxyl group on the central carbon atom) allows this ligand to bind to bone or hydroxyapatite in a tridentate fashion and therefore enhances the sorption of metal–HEDP complexes onto the surface of bone. The relative affinities of metal–HEDP and metal–MDP complexes for calcium(II), hydroxyapatite, and bone are currently under investigation in these laboratories.

Acknowledgments. E.D. gratefully acknowledges financial support from the National Institutes of Health (Grant No. HL-21276) and the Procter & Gamble Co.

References and Notes

(1) Strauss, H. W.; Pitt, B.; James A. E., Jr. "Cardiovascular Nuclear Medicine"; C. V. Mosby: St. Louis, Mo., 1974.
(2) Rhodes, B. A.; Croft, B. Y. "Basics of Radiopharmacy"; C. V. Mosby: St. Louis, Mo., 1978.
(3) Subramanian, G.; Rhodes, B. A.; Cooper, J. F.; Sodd, V. J. "Radiopharmaceuticals"; Society of Nuclear Medicine: New York, 1975.
(4) Deutsch, E. In "Radiopharmaceuticals II"; Society of Nuclear Medicine: New York, 1979.
(5) Siegel, J. A.; Deutsch, E. *Annu. Rep. Inorg. Gen. Synth. 1975* **1976**, 311–326.
(6) Hayes, R. L. In "The Chemistry of Radiopharmaceuticals", Heindel, N. D., Burns, H. D., Honda, T., Brady, L. W. Eds.; Masson: New York, 1978; pp 155–168.
(7) Eckelman, W. C.; Levenson, S. M. *Int. J. Appl. Radiat. Isot.* **1977**, *28*, 67–82.
(8) Keyes, J. W., Jr. "CRC Manual of Nuclear Medicine Procedures", 3rd ed.; CRC Press: Cleveland, Ohio, 1978.
(9) Deutsch, E.; Elder, R. C.; Lange, B. A.; Vaal, M. J.; Lay, D. G. *Proc. Natl. Acad. Sci. U.S.A.* **1976**, *73*, 4287–4289.
(10) DePamphilis, B. V.; Jones, A. G.; Davis, M. A.; Davison, A. *J. Am. Chem. Soc.* **1978**, *100*, 5570–5571.
(11) Smith, J. E.; Byrne, E. F.; Cotton F. A.; Sekutowski, J. C. *J. Am. Chem. Soc.* **1978**, *100*, 5571–5572.
(12) Thomas, R. W.; Estes, G. W.; Elder, R. C.; Deutsch, E. *J. Am. Chem. Soc.*, **1979**, *101*, 4581–4585.
(13) Jones, A.; Francis, M. D.; Davis, M. A. *Semin. Nucl. Med.* **1976**, **6**, 820–825.
(14) Buja, L. M.; Tofe, A. J.; Kulkarni, P. V.; et al. *J. Clin. Invest.* **1977**, *60*, 724–740.
(15) Davis, M. A.; Holman, B. L.; Carmel, A. N. *J. Nucl. Med.* **1976**, *17*, 911–917.
(16) DeLaMatter, D.; McCullough, J. J.; Calvo, C. *J. Phys. Chem.* **1973**, *77*, 1146–1148.
(17) Barnett, B. L.; Strickland, L. C. *Acta Crystallogr. Sect. B* **1979**, *35*, 1212–1214.
(18) Uchtman, V. A.; Gloss, R. A. *J. Phys. Chem.* **1972**, *76*, 1298–1304.
(19) Uchtman, V. A. *J. Phys. Chem.* **1972**, *76*, 1304–1310.

Karen Libson, Edward Deutsch*
Department of Chemistry, University of Cincinnati
Cincinnati Ohio 45221

B. L. Barnett
Miami Valley Laboratories, Procter & Gamble Company
Cincinnati, Ohio 45239

Received November 5, 1979

Shape-Selective Fischer–Tropsch Synthesis Catalyzed by Zeolite-Entrapped Cobalt Clusters

Sir:

Catalyst selectivity is the central problem in Fischer–Tropsch (F–T) synthesis of fuels and petrochemical substitutes from $CO + H_2$.[1] Standard F–T catalysts include supported metals (e.g., Co on silica) typically used at 200–400 °C and 10–200 atm and exhibiting product distributions in the C_1–C_{30} range. Metal clusters are potentially valuable as selective F–T catalysts, having unique structures with neighboring metal centers, but only catalysts of very low activity have been reported.[2] A cobalt complex supported on a polymer was found to be catalytically active for F–T synthesis at 200 °C, but, although it apparently contained unique, stabilized mononuclear metal species, it was unselective, giving products in the C_3–C_{20} range.[3] We have inferred that metal clusters having unique structures and stabilized on a support[4] might provide the sought-for combination of activity and selectivity. Our goal was to extend the class of F–T catalysts to metals supported in zeolites[5]—molecular sieves offering both the prospect of stable encapsulation[6] of metal clusters within the molecular-scale cages and the prospect of shape-selective catalysis.[7,8]

The results summarized here show that zeolite-encapsulated cobalt clusters are the first shape-selective F–T catalysts, also offering the advantages of high activity and stability under conditions of potential commercial significance. The catalysts were prepared by reduction of Co^{2+} ions exchanged into A- and Y-type zeolites.[9]

CoA zeolite has been reported to be a propylene hydroformylation catalyst,[10] but its lack of shape selectivity, indicated by the *n*- to isobutyraldehyde product distribution, suggests that destruction of the alumino-silicate structure occurred, which, we infer, might have resulted from high-temperature reduction of Co^{2+} ions by reactant H_2 inside the zeolite pores during catalysis.[11] Therefore, to prevent "decationization"[5] followed by destruction of the zeolite, we used metal vapors instead of hydrogen as the reducing agent.[12] The products of Cd-vapor reduction of CoA (designated Co^0–CdA) and of CoY (designated Co^0–CdY) were shown by X-ray diffraction to have maintained their zeolitic framework structures.

Results of catalytic reaction experiments with $CO + H_2$ in an isothermal flow reactor are summarized in Table I. *The striking result is that Co^0–CdA catalyzed CO–H_2 conversion at 151 °C and ~6 atm, selectively giving propylene as the only detectable hydrocarbon product* (expt 2). The catalytic activity initially increased for 2–3 h on stream, after which there was no change for 17.5 h, the full period of the experiment. The steady-state conversion was ~1%, and the reaction rate was ~0.4 CO molecules converted/(Co atom h). The initial induction period is suggested to be an indication of the gradual formation of the catalytically active species inside the zeolite cages. The infrared spectrum of the catalyst removed from the reactor after the experiment shows a cobalt carbonyl complex (or a mixture of complexes) (Figure 1); this spectrum suggests the presence of Co clusters with terminal but no bridging carbonyls.[13]

We infer from these results that, at 151 °C, Co^0–CdA acted as a shape-selective F–T catalyst, the active species being cobalt carbonyls (presumably clusters) encapsulated in the ~11-Å pores. The selectivity indicated by the lack of hydrocarbon products other than propylene suggests that nearly uniform cobalt carbonyls were responsible for the catalysis. The Cd ions[14] introduced into the zeolite as a result of the reduction of Co might have played a role in the catalysis.

At a higher reaction temperature, the same catalyst produced propane–propylene mixtures of varying proportions, depending on the CO:H_2 ratio of the reactant stream, and

0002-7863/80/1502-2478$01.00/0 © 1980 American Chemical Society

Table I. Catalytic Conversion of CO + H_2

		activation	reaction conditions[b]				
expt	catalyst	(under H_2 flow, 1 atm),[a] °C, h	temp, °C	total pressure, atm	CO:H_2 mole ratio	hydrocarbon product, mol %	remarks
1	Co^0-CdA	204, 14	182-200	6.2	1:1	propane, ~12 propylene, ~88	fast deactivation accompanied by formation of some C_1
		25, 4	217	5.6	1:24	propane, 30-40 propylene, ~60 undetected product, 0-10	higher conversion, fast deactivation
		250, 6	223	5.4	1:24	propane, 40 propylene, 60	lower conversion
		295, 16	294	5.6	1:24	traces of C_3	
			220-250	6.4	1:1	mainly C_1 traces of C_2, C_3	
			287	6.4	1:1	C_1-C_5	higher conversion
2	Co^0-CdA	200, 5	151	6.5	1:1	propylene, 100	no deactivation during 17.5 h
3	CoA	200, 5	150	6.3	1:1		
			185	6.3	1:1	traces of propylene	
4	Co^0-CdY	200, 9.5	152	6.5	1:1	mainly C_1 traces of C_2-C_4	slightly higher conversion after 5.5 h
			182-183	6.5	1:1	mainly C_1 and C_4-C_6	

[a] The activation steps for the Co^0-CdA catalyst were performed in the order of listing, with the catalytic reaction experiments interspersed as noted. [b] Experiments were carried out with a nearly isothermal reactor operated with nearly a piston flow of reactants. The mass of catalyst was typically 0.5 g and the flow rate of CO + H_2 was in the range 0.10-1.30 cm^3 (STP)/s. The reactant gases were purified to remove traces of water and metal carbonyls. The products were analyzed by gas chromatography.

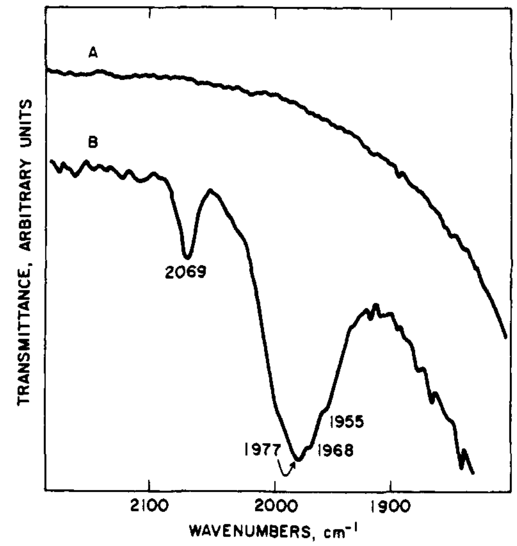

Figure 1. Infrared spectrum of catalyst before (A) and after (B) expt 2 (Table I). The spectra were recorded on a Nicolet 7000 FT IR spectrometer.

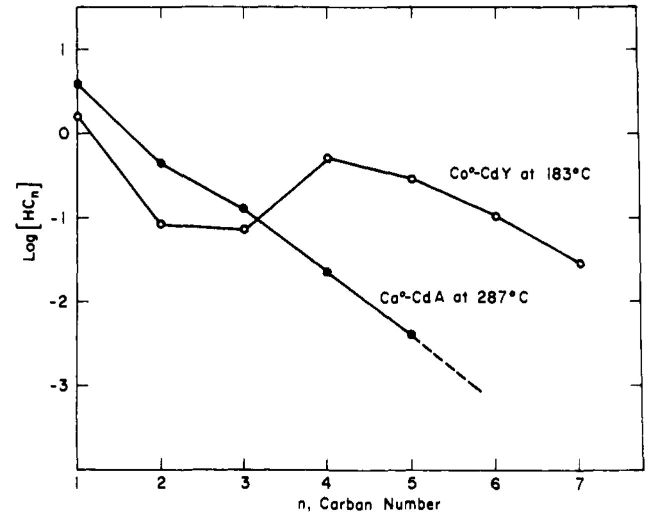

Figure 2. A Schulz-Flory-type plot for Fischer-Tropsch catalysts derived from zeolite-entrapped cobalt clusters. [HC_n] is the linear alkane concentration, in moles per 100 g of total hydrocarbon mixture.

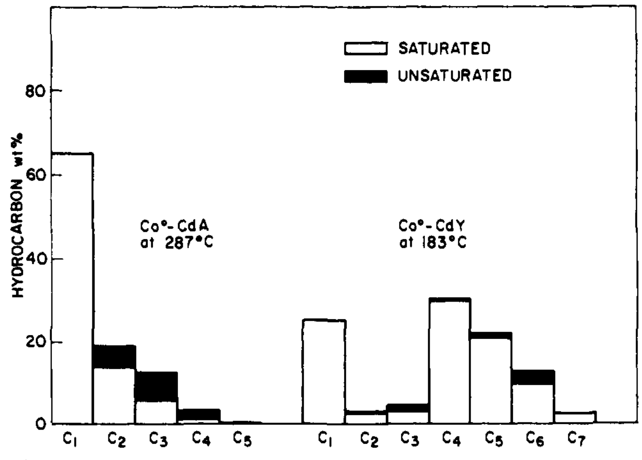

Figure 3. Hydrocarbon product distribution for Fischer-Tropsch catalysts derived from zeolite-entrapped cobalt clusters.

catalyst deactivation occurred over a period of ~5 h (expt 1). After being reactivated in flowing H_2 at 295 °C, the Co^0-CdA catalyst was active at 287 °C (a temperature typically applied with a standard F-T catalyst) for formation of a C_1-C_5 hydrocarbon mixture [representative of a typical F-T catalyst (Figures 2 and 3)].[15] The ordinary Schulz-Flory product distribution observed at this stage implies that the Co species migrated out of the micropores and sintered to give larger Co particles which behaved like those of typical F-T catalysts.

In contrast, unreduced CoA was inactive at 150 °C, and at 185 °C produced only traces of propylene, probably as a result of slow reduction of Co^{2+} ions by H_2 to give traces of the catalytically active metal carbonyl(s) (Table I, expt 3).

The larger cages (supercages) in Co^0-CdY zeolite are expected to have allowed formation of larger Co clusters, and the larger pores are expected to have evidenced less marked shape selectivity than those of Co^0-CdA. Indeed, no propylene was formed from CO + H_2 at 152 °C, but at 182 °C the catalyst was active, giving C_1–C_7 hydrocarbon mixtures at a conversion of ≥15% and a rate of ~8 molecules of CO converted/(Co atom h). *Most strikingly, almost no C_2 or C_3 hydrocarbons were produced, the main product being n-butane, with the C_4–C_7 mixture constituting ≃70% of the hydrocarbon product* (Figure 3). The deviation from Schulz–Flory behavior (Figure 2) and the sharp product concentration profile (~25% C_4, ~0% C_8) confirm a shape selectivity different from that observed with the A-type zeolite. The size, structure, and environment of the catalytically active species are evidently important in addition to the molecular-sieving character of the zeolite pores.

We believe that these results may portend a challenging new chemistry of stabilized metal clusters in the unique solvent-like environments of zeolite pores and open the way to new catalytic science and technology to meet some of our most pressing needs for synthesis gas conversion into fuels and petrochemical substitutes.

Acknowledgment. We thank A. W. Sleight, E. Gleason, and P. Gajardo for helpful discussions.

References and Notes

(1) For recent reviews see C. Masters, *Adv. Organomet. Chem.*, **17**, 61 (1979); M. A. Vannice, *Catal. Rev.-Sci. Eng.*, **14**, 153 (1976).

(2) M. G. Thomas, B. F. Beier, and E. L. Muetterties, *J. Am. Chem. Soc.*, **98**, 1297 (1976); G. C. Demitras and E. L. Muetterties, *ibid.*, **99**, 2796 (1977).

(3) P. Perkins and K. P. C. Vollhardt, *J. Am. Chem. Soc.*, **101**, 3985 (1979).

(4) R. Pierantozzi, K. J. McQuade, B. C. Gates, M. Wolf, H. Knözinger, and W. Ruhmann, *J. Am. Chem. Soc.*, **101**, 5436 (1979); J. J. Rafalko, J. Lieto, B. C. Gates, and G. L. Schrader, Jr., *J. Chem. Soc., Chem. Commun.*, 540 (1978); S. C. Brown and J. Evans, *ibid.*, 1063 (1978); A. K. Smith, A. Theolier, J. M. Basset, R. Ugo, D. Commereuc, and Y. Chauvin, *J. Am. Chem. Soc.*, **100**, 2590 (1978); J. Lieto and B. C. Gates, *Chemtech*, in press.

(5) For a review of zeolite structure and chemistry, see D. W. Breck, "Zeolite Molecular Sieves", Wiley-Interscience, New York, 1974.

(6) The idea of encapsulating metal clusters in zeolites follows from the idea of high-pressure gas encapsulation, which has potential value for hydrogen storage: D. Fraenkel and J. Shabtai, *J. Am. Chem. Soc.*, **99**, 7074 (1977); D. Fraenkel, *Chemtech*, in press.

(7) For a review of shape-selective catalysis by zeolites, see S. M. Csicsery in "Zeolite Chemistry and Catalysis", J. A. Rabo, Ed., the American Chemical Society, Washington, D.C., 1976, p 680.

(8) Metal carbonyls and metal cluster carbonyls have been introduced into Y-type zeolites [P. Gallezot, G. Coudurier, M. Primet, and B. Imelik in "Molecular Sieves-II", J. R. Katzer, Ed., the American Chemical Society, Washington, D.C., 1977, p 144; P. Gelin, Y. Ben Taarit, and C. Naccache, *J. Catal.*, **59**, 357 (1979); D. Ballivet-Tkatchenko and G. Coudurier, *Inorg. Chem.*, **18**, 558 (1979)] and produced inside zeolite cages [M. Primet, J. C. Verdine, and C. Naccache, *J. Mol. Catal.*, **4**, 411 (1978); E. Mantovani, N. Palladino, and A. Zanobi, *ibid.*, **3**, 285 (1977/1978)]. Evidently, the metal carbonyls became encapsulated within the supercages. Some of these metal-containing zeolites show catalytic activity for F–T synthesis, but only at high temperatures (≥250 °C) and with no apparent selectivity [D. Ballivet-Tkatchenko, G. Coudurier, H. Mozzanega, I. Tkachenko, and A. Kiennemann, *J. Mol. Catal.*, **6**, 293 (1979)]. Recently, however, a reduced RuY zeolite has been reported to be an active F–T catalyst exhibiting a nonlinear Schulz–Flory distribution of products and a drastic decline in chain growth probability above C_{10}, a phenomenon attributed to a "cage effect" [H. H. Nijs, P. A. Jacobs, and J. B. Uytterhoeven, *J. Chem. Soc., Chem. Commun.*, 180 (1979)]. Earlier, a rhodium carbonyl cluster entrapped in zeolite Y was reported (Mantovani et al., cited above) to catalyze olefin hydroformylation, but no shape selectivity was found.

(9) The cation exchange of commercial zeolites 5A and SK-41 (HY) (Linde) was carried out with 0.1 N $CoCl_2$ solutions at ~95 °C until equilibrium was attained. Cd vapor treatment of the dried samples was performed at 450–500 °C, and the excess of Cd was removed by evacuation of the reduced samples at >450 °C. The blue unreduced samples became gray-black after reduction and removal of the unreacted Cd. It is not known whether the reduction of Co^{2+} to Co^0 was complete.

(10) P. Centola, G. Terzaghi, R. Del Rosso, and I. Pasquon, *Chim. Ind.* (*Milan*), **54**, 775 (1972).

(11) Destruction of A zeolite can result from formation of "hydrogen" zeolite followed by thermal dehydration involving framework oxygens.[5]

(12) Metal vapor reduction of exchangeable cations in zeolite A was first performed by R. M. Barrer and J. L. Whiteman [*J. Chem. Soc. A*, 19 (1967)], who reduced Ag^+ in AgA by Hg vapor. Most of the reduced Ag was reported to have escaped from the zeolite intracrystalline channel system and agglomerated to form large particles external to the zeolite micropores. Co^0 is potentially a better catalyst than Ag^0 and is also much less mobile in zeolite A than Ag^0, but Hg vapors are not sufficiently effective as a reducing agent for Co^{2+} ions. Therefore, we have chosen CoA with Cd as the reducing agent.

(13) Only the catalyst recovered from expt 2 (Table I) showed infrared Co–CO absorption bands (Figure 1). It is noteworthy that no particular care was taken to protect the catalyst from the ambient atmosphere.

(14) Recently, the crystal structure of Cd(II)-exchanged zeolite A evacuated at 500 °C was reported: L. B. McCusker and K. Seff, *J. Am. Chem. Soc.*, **101**, 5235 (1979). Upon exposure of the zeolite to Cd vapor, Cd^+ and Cd_2^{2+} species were formed within the cages. We believe that in our case a similar system might have formed and Cd species, whether alone or combined with Co,[12] could participate in the catalytic action, as predicted by McCusker and Seff.

(15) Metal migration outside the micropores of zeolite A at temperatures >200 °C was proposed to explain the change in shape selectivity in the case of catalytic olefin hydrogenation with NiA which had been reduced by Na in liquid NH_3 under mild conditions: H. Minchev and F. Steinbach, *Proc. Int. Conf. Mol. Sieves, 3rd, 1973*, 410 (1973).

Dan Fraenkel, Bruce C. Gates*
Center for Catalytic Science and Technology
Department of Chemical Engineering
University of Delaware, Newark, Delaware 19711

Received December 3, 1979

Platinum(II) Anti-Tumor Agents. A New Class of Intrastrand Cross-Linking Models Exhibiting Significant Intracomplex Base–Base Interactions

Sir:

The anti-tumor agent *cis*Pt {*cis*-[$(NH_3)_2PtCl_2$]} has exhibited remarkable clinical utility against a broad spectrum of human tumors.[1] Since the discovery of the anti-tumor activity of Pt(II) compounds,[1] a considerable amount of research has focused on elucidating the mechanism of activity of these novel drugs. Almost all of the evidence accumulated to date implicates DNA of the tumor cell as the molecular target of *cis*Pt.[2] Although numerous reaction sites are available on a polynucleotide,[3] strong evidence exists that at low Pt/DNA ratios (conditions best approximating in vivo levels) the guanine bases are attacked preferentially.[3] A compelling and chemically feasible, but unproven, explanation for the requirement of two cis positions on all active Pt(II) anti-tumor agents is that an intrastrand cross-link between two guanosine bases is the critical lesion. Evidence for such cross-linking in polynucleotides has been reported.[2-4]

An alternative explanation for the requirement of two cis leaving groups is that an N(7),O(6) chelate is formed between the guanine base and the Pt(II) center.[5] This hypothesis is attractive since, by involving the 6-oxo group in the interaction with an electrophilic center, the model affords a mechanism for base mispairing and thereby an explanation for the effectiveness of the Pt(II) agent.[5] However, no definitive structural evidence exists for such a chelation mode in Pt(II) chemistry.[6]

In contrast, intrastrand cross-linking models containing Pt(II) and guanosine[7-8] (class I) or the dianion of inosine 5′-monophosphate (5′-IMP)[9-12] (class II) are known. However, quite different structural features are found in these two classes of complexes (Table I). The molecular structures of the closely related bis(guanosine) complexes[7-8] contain no unusual features. On the other hand, the molecular structures of the bis(5′-IMP) complexes show appreciable intracomplex base–base interactions.[9-12] Evaluation of these interactions in the 5′-IMP systems is complex since the compounds are isomorphous with the monosodium salt of 5′-IMP (NaH-IMP),[13] and the crystal structure (particularly the binding of the Na^+ counterion) is important.

In this report, we describe the preparation and structure of the complex [(tn)Pt(Me-5′-GMP)$_2$], where tn = trimethylenediamine and Me-5′-GMP is the phosphate methyl ester of guanosine 5′-monophosphate (Figure 1). This neutral complex lacks any charge compensating counterion, allowing a freer environment in the solid than in the Pt(II)-5′-IMP

0002-7863/80/1502-2480$01.00/0 © 1980 American Chemical Society